STUDY OF QUENCH MARGINS FOR BETATRON HALO LOSSES WITH NEW HL-LHC COLLIMATION OPTICS

N. Duarte*, R. Bruce, L. S. Esposito, H. Guérin, A. Lechner, B. Lindstrom, S. Redaelli, V. Rodin
CERN, Geneva, Switzerland

Abstract

The High-Luminosity Large Hadron Collider (HL-LHC) will mark a new phase of LHC operation, aiming to reach an integrated luminosity of 3000 fb^{-1} over 10 years of operation. A key element to achieve this target is the beam intensity increase, nearly doubling the number of protons per bunch compared to the initial LHC design. This increases the load on the collimators protecting against beam losses, particularly in the betatron cleaning insertion region (IR7), a multistage collimation system responsible for beam halo cleaning. Particles intercepted here may undergo diffractive scattering and propagate for hundreds of meters, reaching the adjacent dispersion suppressor (DS) sections.

To assess the impact of these losses, FLUKA simulations have been performed to predict the power deposition in the superconducting DS magnets on both sides of IR7. Accurate modeling of these losses is essential to ensure safe machine operation and to optimize beam loss monitor thresholds, minimizing unnecessary protective beam dumps.

In this contribution, we present shower simulation studies for the latest HL-LHC collimation optics (v1.6), with improved cleaning and impedance in IR7, and compare them to the previous one (v1.5).

INTRODUCTION

Run 4 of the LHC, scheduled to start in 2030 after the completion of Long Shutdown 3 (LS3), will mark the beginning of the High-Luminosity LHC (HL-LHC) proton-proton operation, and will already bring an increase of the levelled peak luminosity from 2.2×10^{34} cm^{-2} s^{-1} achieved during Runs 2 and 3 to about 5×10^{34} cm^{-2} s^{-1}, with a possible further increase in later years, ultimately reaching 7.5×10^{34} cm^{-2} s^{-1} [1]. This luminosity is intentionally limited through luminosity levelling to reduce event pile-up in the detectors, which in turn allows for longer fills [2].

The increase in luminosity is achieved through improvements on multiple fronts across the accelerator complex: the total number of protons circulating in each beam will be nearly doubled compared to the original design parameters, an upgrade of the inner triplet magnets at insertion regions IR1 (ATLAS) and IR5 (CMS) will provide reduced beam sizes by means of stronger focusing [3], and the installation of crab-cavities (also in IR1 and IR5) which rotate the proton bunches to maximize the overlap of the colliding beams [4].

To mitigate impedance-induced instabilities and accommodate higher luminosity and new experimental layouts, the HL-LHC upgrade includes the installation and replacement of multiple collimators [5]. Monte Carlo simulations are fundamental for optimizing collimation configurations [6] and assessing the quench margin with higher beam intensities in the HL-LHC era. Beam tracking simulations are used to model the dynamics of halo particles and to estimate where the most critical losses around the ring occur [7]. This information is then used as input for particle–matter interaction simulations, modelling the development of hadronic and electromagnetic showers in the accelerator components, allowing to predict localized energy depositions in sensitive elements, such as superconducting magnet coils [8, 9].

In this work, we study the impact of betatron halo losses, leaking out of the collimation system, on the dispersion suppressor (DS) magnets adjacent to the betatron cleaning insertion region IR7 using the latest HL-LHC collimation optics (v1.6), with increased beta functions in IR7 allowing for larger physical collimator gaps and reduced impedance [10]. The results are compared with those for the previous HL-LHC baseline optics version (v1.5).

HL-LHC COLLIMATION SYSTEM

The energy stored in each of the HL-LHC colliding beams, around 680 MJ, requires careful control of beam losses to prevent quenches of superconducting magnets. Of particular concern are the niobium-titanium (NbTi) coils of the LHC dipole magnets, operating at a temperature of 1.9 K, and in the immediate surrounding of the beam pipes. Local energy deposition from lost protons and secondary particles can induce a heating effect and increase the coil temperature beyond the critical value, resulting in a magnet quench, which may lead to several hours of downtime until proper cryogenic conditions are restored. To mitigate this, beam losses must be carefully monitored and controlled.

The LHC collimation system was designed to withstand beam lifetimes as low as 12 min, sustained for up to 10 s, at 7 TeV energy. This requirement is maintained for the HL-LHC, implying that collimators must be able to cope with higher power losses due to the higher beam intensity [11].

To achieve efficient cleaning, the LHC employs two complementary cleaning insertions: momentum cleaning in IR3 and betatron cleaning in IR7. Both regions use a multistage collimation hierarchy in which primary collimators are positioned closest to the beam, intercepting most of the halo particles with large transverse amplitudes. Particles scattered at the primary collimators (TCPs) generate particle showers that are subsequently intercepted by secondary collimators (TCSs) and active shower absorbers (TCLAs).

The main bottleneck of the LHC regarding collimation leakage are the dispersion suppressor (DS) sections on both

* Work supported by the High Luminosity LHC project.
Corresponding author: nuno.duarte@cern.ch

Table 1: IR7 collimator apertures for tight/relaxed settings.

Collimator	Number per beam	Half-gaps (σ)	
		tight	relaxed
Primary (TCP)	3	6.7	8.5
Secondary (TCS)	11	9.1	10.1
Absorber (TCLA)	5	12.7	14.0

ends of IR7, where losses in cold regions are among the highest. A fraction of particles interacting with the collimator jaws undergo single diffractive scattering, resulting in protons with slightly reduced momentum that may travel several hundreds of meters without being intercepted by any other collimators, eventually being lost in the superconducting magnets of the DS, where dispersion begins to rise.

OPTICS AND COLLIMATION SETTINGS

The IR7 collimation hierarchy consists of a sequence of 3 TCPs, 11 TCSs, and 5 TCLAs. To ensure efficient cleaning in both planes, collimators are installed with horizontal, vertical, and varying skew orientations. Their layout and apertures are symmetric for both beam 1 and beam 2.

Along with different optics, also distinct collimation configurations are considered in HL-LHC studies: tight settings for better halo cleaning, and relaxed settings for improved impedance. The values of the half-gaps (distance between each jaw and the reference orbit) for both configurations are shown in Table 1. Half-gaps are expressed in terms of rms of transverse beam size, which, for a given plane and neglecting dispersion, is related to beam emittance ϵ, and beta function β, at any point s along the reference beam orbit by $\sigma(s) = \sqrt{\epsilon\,\beta(s)}$, allowing to define a gap that scales with beam parameters and optical functions. A design value of ϵ=2.5 µm is used to calculate HL-LHC collimator settings.

Due to their low electric conductivity and proximity to the beam, adopting apertures of a few millimeters, collimators account for roughly half of the overall impedance [5]. The effect of impedance gives rise to self-induced electromagnetic fields which affect beam stability, a concern that becomes even more critical for the higher beam intensities of HL-LHC. To mitigate this, the upgrade program includes dedicated measures to reduce the machine impedance. On one side, a reduction of the impedance will be achieved by replacing 2 primary and 9 secondary collimators (per beam) with new lower impedance ones, based on a newly developed MoGr (molybdenum–graphite) composite with a Mo coating [12]. Part of this upgrade was already implemented in LS2, with 5 secondary collimators per beam still to be replaced in LS3 [13]. In addition to hardware upgrades, a new optics design (v1.6) has been developed to further reduce impedance by increasing the beta functions in the IR7 collimation region [10], allowing for larger collimator gaps while preserving the σ half-gap values of optics v1.5.

While initial studies indicated improved cleaning performance with the new optics [14], dedicated simulations for particle–matter interaction are required to evaluate the effects of particles reaching the IR7 DS sections, particularly the power density deposited in superconducting magnet coils, allowing to assess quench margins. These simulations were conducted for both v1.5 and v1.6 optics using the Monte Carlo FLUKA code [15–17]. Relaxed collimation settings were considered for both optics versions, as these generate higher power deposition in the DS magnets [18]. The layout and orientation of collimators is the same for both optics versions, changing only the magnetic strengths across the lattice and the collimators half-gap.

SIMULATION RESULTS

A multi-step simulation method is adopted to evaluate the power deposition originating from collimation losses in IR7. In a first stage, the six-dimensional phase-space distribution (position and momentum) of particles lost at the collimators is determined from multi-turn tracking simulations performed with SixTrack [19], along with FLUKA code to handle particle interactions with the collimators. This approach, referred to as SixTrack–FLUKA coupling [20,21], is a computationally efficient way to enable the realistic tracking of particles over many turns while accurately accounting

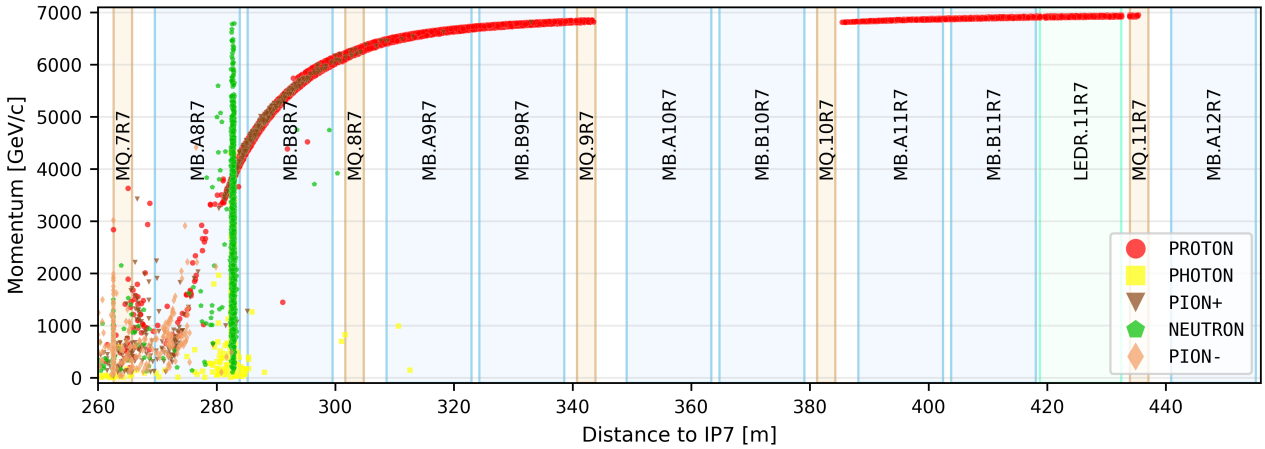

Figure 1: Momentum and longitudinal coordinate of particles exiting the beam pipe in the DS region for v1.6 optics.

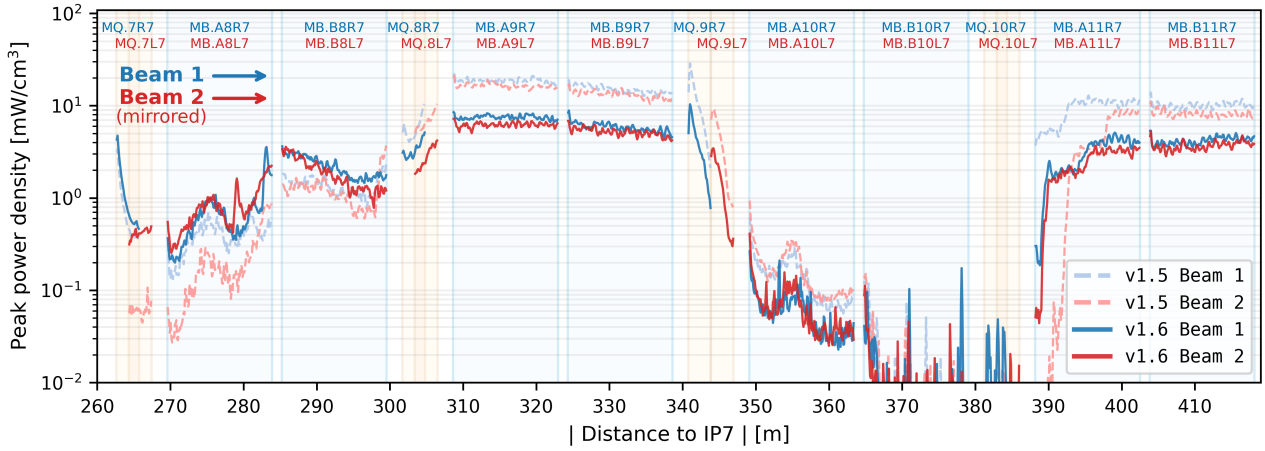

Figure 2: Peak power density scored along the length of the IR7 DS magnets for both beams and optics versions.

for the physical processes occurring when particles traverse the collimator jaws, where they may undergo an inelastic interaction, or be scattered back to the beam pipe to continue to be tracked. The distribution of protons impacting on the collimators is used as input for the FLUKA simulations.

The long extension and complexity of the geometry to be simulated in FLUKA makes a manual implementation unfeasible. To overcome this, the LineBuilder [22, 23] tool is used, allowing to automatically and dynamically place FLUKA models of accelerator components, set magnetic fields, and define scoring regions, profiting from the lattice capability of FLUKA to replicate elements. To optimize computation time, simulations are split in a 2-step approach. In the first step, the phase-space distributions of protons lost in the collimators are loaded and transported along with generated secondaries only up to a high energy threshold (order of hundreds of GeV). Particles falling below this threshold are discarded, while those that manage to reach the DS are saved by dumping their energy and phase-space coordinates. A visual representation of the output of the first simulation step for beam 1 is presented in Figure 1, showing the longitudinal position and momentum of particles lost in the DS region. A narrow loss peak in dipole MB.A8R7 is observed due to neutrons and photons which are not deflected by the magnetic field and travel in a straight trajectory until they are intercepted by the dipole arc. Positive pions of similar momentum have the same magnetic rigidity as protons, and thus are able to reach the first pair of dipoles, before eventually decaying. After this point, essentially only protons close to the nominal 7 TeV momentum progress further into the DS. A gap in losses is observed for the dipoles of cell 10R7 due to the horizontal focusing of quadrupole MQ.9R7, which is then counteracted by the defocusing effect of MQ.10R7.

The information of the particles reaching the DS is used as input for the second step, in which particles are transported down to low energies, allowing for showers to fully develop, and their energy deposition to be precisely scored. Figure 2 shows, for both beams and optics, the peak power density deposited in the inner coils of the DS superconducting magnets across their longitudinal dimension. Cylindrical bins are used to score the inner magnet coils, and the peak power for each longitudinal bin is defined as the maximum over the radially averaged angular bins. Simulation data was normalized for a 1 MW loss scenario, corresponding to a beam lifetime of 12 min at 7 TeV, yielding a loss rate of 8.81×10^{11} p/s.

Similarly to the findings obtained in studies with previous LHC optics [24, 25], the pair of dipoles in cells 9R7 and 9L7 are the most critical elements in terms of quench risk. However, a substantial reduction is observed for the new optics version v1.6, with the peak power density dropping from a maximum of ~20 mW cm^{-3} to ~10 mW cm^{-3}. An analysis of the interaction history of particles reaching the DS shows that this reduction is attributed to a more effective interception of slightly off-momentum protons from single diffractive interactions at the primary collimators by the downstream collimators, as a result of the new IR7 optics.

Previous experimental studies at 6.5 TeV have measured quench levels of NbTi dipole magnets to be in the range of 15–20 mW cm^{-3} [26, 27], with more recent measurements at 6.8 TeV indicating a slight reduction (~10 %), a trend which is expected to be maintained also at 7 TeV. Consequently, while one cannot fully exclude a magnet quench with v1.5 optics, the margin becomes more comfortable for v1.6.

CONCLUSION

HL-LHC optics v1.6 incorporates new IR7 optics for proton collimation, designed to improve cleaning performance and machine impedance. This study confirms an overall reduction of power deposition in the IR7 DS, decreasing by roughly a factor of 2 for the most critical magnets, peaking at ~10 mW cm^{-3}. These findings indicate that v1.6 optics provide increased quench margins for the IR7 DS magnets during HL-LHC operation.

REFERENCES

[1] R. De Maria *et al.*, "High Luminosity LHC optics scenarios for Run 4", in *Proc. IPAC'23*, Venice, Italy, May 2023, pp. 602–605. doi:10.18429/JACoW-IPAC2023-MOPL034

[2] B. Muratori and T. Pieloni, "Luminosity levelling techniques for the LHC", in *Proc. ICFA Mini-Workshop on Beam-Beam Effects in Hadron Colliders*, Geneva, Switzerland, Mar. 2014, pp. 177–181. doi:10.5170/CERN-2014-004.177

[3] M. Zerlauth and O. Bruning, "Status and prospects of the HL-LHC project", in *Proc. Conf. High Energy Physics 2023*, Hamburg, Germany, Aug. 2023, p. 615. doi:10.22323/1.449.0615

[4] S. Verdú-Andrés *et al.*, "Design and vertical tests of double-quarter wave cavity prototypes for the high-luminosity LHC crab cavity system", *Phys. Rev. Accel. Beams*, vol. 21, no. 8, p. 082002, 2018. doi:10.1103/PhysRevAccelBeams.21.082002

[5] O. Brüning and L. Rossi, "The High Luminosity Large Hadron Collider – HL-LHC", in *The High Luminosity Large Hadron Collider*. World Scientific, 2024, pp. 1–53. doi:10.1142/9789811278952_0001

[6] O. Aberle *et al.*, "High-luminosity Large Hadron Collider (HL-LHC): Technical Design Report", CERN, Geneva, Switzerland, Rep. CERN-2020-010. doi:10.23731/CYRM-2020-0010

[7] A. Donadon Servelle *et al.*, "An evaluation of collimation settings for the High Luminosity LHC baseline", in *Proc. IPAC'25*, Taipei, Taiwan, Jun. 2025, pp. 2532–2535. doi:10.18429/JACoW-IPAC2025-THPB015

[8] E. Skordis *et al.*, "Study of the 2015 top energy LHC collimation quench tests through an advanced simulation chain", in *Proc. IPAC'17*, Copenhagen, Denmark, May 2017, pp. 100–103. doi:10.18429/JACoW-IPAC2017-MOPAB012

[9] A. Lechner *et al.*, "Validation of energy deposition simulations for proton and heavy ion losses in the CERN Large Hadron Collider", *Phys. Rev. Accel. Beams*, vol. 22, no. 7, p. 071003, 2019. doi:10.1103/PhysRevAccelBeams.22.071003

[10] B. Lindström *et al.*, "Mitigating collimation impedance and improving halo cleaning with new optics and settings strategy of the HL-LHC betatron collimation system", in *Proc. HB'23*, Geneva, Switzerland, Apr. 2023, pp. 183–187. doi:10.18429/JACoW-HB2023-TUC4C2

[11] S. Redaelli *et al.*, "Collimation of HL-LHC beams", in *The High Luminosity Large Hadron Collider*. World Scientific, 2024, pp. 225–254. doi:10.1142/9789811278952_0008

[12] F. Carra *et al.*, "Mechanical robustness of HL-LHC collimator designs", *J. Phys. Conf. Ser.*, vol. 1350, no. 1, p. 012083, Nov. 2019. doi:10.1088/1742-6596/1350/1/012083

[13] A. Mereghetti, R. Bruce, N. Fuster-Martínez, D. Mirarchi, and S. Redaelli, "Collimation system upgrades for the High Luminosity Large Hadron Collider and expected cleaning performance in Run 3", in *Proc. IPAC'19*, Melbourne, Australia, May 2019, pp. 681–684. doi:10.18429/JACoW-IPAC2019-MOPRB051

[14] B. Lindström *et al.*, "High Luminosity LHC collimation system performance for different optics configurations", in *Proc. IPAC'25*, Taipei, Taiwan, Jun. 2025, pp. 663–666. doi:10.18429/JACoW-IPAC2025-MOPS029

[15] FLUKA website, `fluka.cern`

[16] C. Ahdida *et al.*, "New capabilities of the FLUKA multi-purpose code", *Front. Phys.*, vol. 9, p. 788253, 2022. doi:10.3389/fphy.2021.788253

[17] G. Battistoni *et al.*, "Overview of the FLUKA code", *Ann. Nucl. Energy*, vol. 82, pp. 10–18, 2015. doi:10.1016/j.anucene.2014.11.007

[18] V. Rodin *et al.*, "Power deposition studies for betatron halo losses in HL-LHC", in *Proc. IPAC'23*, Venice, Italy, May 2023, pp. 610–613. doi:10.18429/JACoW-IPAC2023-MOPL036

[19] R. De Maria *et al.*, "SixTrack version 5: status and new developments", in *Proc. IPAC'19*, Melbourne, Australia, Jun. 2019, pp. 3200–3203. doi:10.18429/JACoW-IPAC2019-WEPTS043

[20] A. Mereghetti *et al.*, "SixTrack-Fluka active coupling for the upgrade of the SPS scrapers", in *Proc. IPAC'13*, Shanghai, China, May 2013, pp. 2657–2659.

[21] E. Skordis *et al.*, "FLUKA coupling to Sixtrack", in *ICFA Mini-Workshop on Tracking for Collimation in Particle Accelerators*, vol. 30, Geneva, Swizterland, Oct. 2015, pp. 17–25. doi:10.23732/CYRCP-2018-002.17

[22] A. Mereghetti, V. Boccone, F. Cerutti, R. Versaci, and V. Vlachoudis, "The FLUKA Linebuilder and element database: tools for building complex models of accelerator beam lines", in *Proc. IPAC'12*, New Orleans, LA, USA, May 2012, pp. 2687–2689.

[23] FLUKA LineBuilder tool, `fluka . cern / tools / linebuilder`

[24] C. Bahamonde Castro, "Energy deposition from collimation losses in IR7 dispersion suppressor", unpublished. `indico.cern.ch/event/742082/contributions/3085132/`

[25] A. Waets *et al.*, "Power deposition in superconducting dispersion suppressor magnets downstream of the betatron cleaning insertion for HL-LHC", in *Proc. IPAC'21*, Campinas, SP, Brazil, May 2021, pp. 37–40. doi:10.18429/JACoW-IPAC2021-MOPAB001

[26] M. Schaumann, J. M. Jowett, C. Bahamonde Castro, R. Bruce, A. Lechner, and T. Mertens, "Bound-free pair production from nuclear collisions and the steady-state quench limit of the main dipole magnets of the CERN Large Hadron Collider", *Phys. Rev. Accel. Beams*, vol. 23, no. 12, p. 121003, 2020. doi:10.1103/PhysRevAccelBeams.23.121003

[27] J.-B. Potoine *et al.*, "Power deposition studies for standard and crystal-assisted heavy ion collimation in the CERN Large Hadron Collider", *Phys. Rev. Accel. Beams*, vol. 26, no. 9, p. 093001, 2023. doi:10.1103/PhysRevAccelBeams.26.093001